Journal of Power Sources 221 (2013) 419–426

Contents lists available at SciVerse ScienceDirect

Journal of Power Sources

journal homepage: www.elsevier.com/locate/jpowsour

Investigation of different binding agents for nanocrystalline anatase TiO_2 anodes and its application in a novel, green lithium-ion battery

Arianna Moretti [a,b], Guk-Tae Kim [b], Dominic Bresser [b,*], Katrin Renger [b], Elie Paillard [b], Roberto Marassi [a], Martin Winter [b], Stefano Passerini [b,*]

[a] School of Science and Technology, Chemistry Division, University of Camerino, Via S. Agostino1, I-62032 Camerino (MC), Italy
[b] Institute of Physical Chemistry & MEET Battery Research Centre, University of Muenster, Corrensstr. 28/30 & 46, 48149 Muenster, Germany

HIGHLIGHTS

- Effect of different binders on the electrochemical performances of anatase TiO_2 electrodes.
- Superior electrochemical performance of TiO_2 electrodes comprising CMC or CMC/SBR.
- Cyclability of Li-ion cell comprising TiO_2 and $LiNi_{1/3}Mn_{1/3}Co_{1/3}O_2$ electrodes prepared via aqueous process.

ARTICLE INFO

Article history:
Received 10 June 2012
Received in revised form
27 July 2012
Accepted 31 July 2012
Available online 21 August 2012

Keywords:
TiO_2
Anatase
NMC
Binder
CMC
Lithium-ion full cell

ABSTRACT

The electrochemical performance of nanocrystalline anatase TiO_2 electrodes made using sodium carboxymethyl cellulose (CMC) binder, alone and in combination with styrene butadiene rubber (SBR), has been investigated. The electrochemical behavior of these electrodes, which were made via a water-based process, has been compared with those of electrodes manufactured using traditional polyvinylidene difluoride (PVDF) and its copolymer with hexafluoropropylene (PVDF-HFP) in N-methyl-2-pyrrolidone solution. Without the need of any post coating treatment, such as roll pressing, CMC and CMC/SBR based electrodes possess higher specific capacity, rate capability, and cycling stability than those prepared using PVDF or PVDF-HFP as binding agent. Using the same water based process, CMC based $LiNi_{1/3}Mn_{1/3}Co_{1/3}O_2$ (NMC) electrodes have been prepared.

The combination of CMC based TiO_2 and NMC electrodes in a lab-scale lithium-ion full cell showed a stable cycling performance with a total energy density of more than 120 Wh kg^{-1}. These results demonstrate that anatase TiO_2 is an attractive candidate for the development of safer and greener lithium-ion batteries for future application in hybrid and electric vehicles and stimulate further research on this full lithium-ion cell combination.

1. Introduction

During the last years the market for lithium-ion batteries has been steadily increasing. A further is presently forecasted due to the high energy and power density of this battery chemistry, making it the most promising power source for vehicle applications as well as for stationary energy storage devices for renewable energy sources, such as wind and solar power. However, for these types of applications a further decrease in production cost and improvements in terms of environmentally friendliness, safety, as well as end of life recyclability are strongly required [1]. Presently, commercially available lithium-ion batteries mostly comprise a graphite anode and a lithium cobalt oxide ($LiCoO_2$) cathode. Nevertheless, $LiCoO_2$ is expensive, environmentally harmful, toxic, and suffers of chemical instability at high potentials, leading, in worst cases, to thermal runaway and explosion of the cell [2]. Moreover, the use of graphite on the anode side causes severe safety issues, since it operates close to the Li^+/Li redox couple with a potential risk of metallic lithium plating and dendrite formation when the cell is overcharged. In addition, graphite suffers a rather high irreversible capacity loss during the initial cycles due to the formation of a solid electrolyte interphase (SEI) resulting from electrolyte decomposition [3,4]. SEI is, however, indispensable for protecting the graphite surface to avoid continuous direct contact with the solvent, which would result in an ongoing electrolyte decomposition reaction.

As safety is one of the major issues in large scale applications of lithium-ion batteries, alternative electrode materials with enhanced electrochemical performance in terms of energy and

* Corresponding authors. Tel.: +49 251 8336618; fax: +39 (0) 630486357.
E-mail addresses: Dominic.bresser@uni-muenster.de (D. Bresser), stefano.passerini@uni-muenster.de (S. Passerini).

0378-7753/$ – see front matter © 2012 Elsevier B.V. All rights reserved.
http://dx.doi.org/10.1016/j.jpowsour.2012.07.142

power density, improved efficiency, low cost, and environmentally sustainability are strongly required.

Among a variety of possible anode materials, titanium based compounds are currently considered as potential graphite substitutes [5,6]. Among these, particularly anatase TiO_2 has attracted increasing scientific and commercial interest due to its natural abundance, low cost, environmentally friendliness, and biocompatibility. The utilization of anatase TiO_2 as anode material for lithium-ion batteries leads to significant improvements in terms of safety, since lithium ion (de-)insertion takes place at a potential around 1.7 V *vs.* Li^+/Li, thus reducing, if not eliminating, the risk of lithium plating and dendrite formation in case of accidental overcharge [1,7–9]. The theoretical specific capacity of TiO_2, corresponding to the reversible lithium uptake and release of one lithium ion per formula unit of oxide, is 335 mAh g^{-1}, and hence very close to that of graphite. However, the practically available capacity of micrometer-sized TiO_2 is limited to only 168 mAh g^{-1} according to the reversible uptake and release of merely 0.5 lithium per TiO_2 [7,8]. Recent studies have reported that the electrochemical properties of this material are strongly affected by its particle size and morphology [10–12]. The practical limitation, in terms of high rate capability and specific capacity, could be overcome by decreasing the particle size or increasing the specific surface area of anatase TiO_2 by utilizing for instance highly mesoporous structures or nano-sized particles. Very promising results have been obtained for example by using nanosized one-dimensional anatase TiO_2 nanorods embedded in a percolating carbonaceous matrix, which have shown a specific capacity as high as 210 mAh g^{-1} at 1 C (corresponding to a composition of $Li_{0.63}TiO_2$) as well as enhanced high rate capability [13]. However, due to the rather high lithium (de-) insertion potential of anatase TiO_2, a suitable cathode material operating at rather high voltage is required, in order to achieve a competitive overall energy density for final lithium-ion cells. $LiNi_{1/3}Mn_{1/3}Co_{1/3}O_2$ (NMC), operating at high potential (4.3 V), which is already used in commercial applications, is less toxic and cheaper than the isostructural $LiCoO_2$, and hence appears as a suitable candidate for full lithium-ion cells comprising TiO_2 [14,15]. In general, for further advances in the development of safer and greener batteries, however, all electrode components as well as their production processes need to be considered. Beside the active materials, the binder plays a significant role. Currently, most batteries contain fluorinated binders as polyvinylidene difluoride (PVDF) and its copolymers, which necessitate the use of organic solvents as N-methyl-2-pyrrolidone (NMP) for the slurry preparation. These binders ensure a rather high mechanical strength and flexibility of the final electrodes and provide adhesion of the active material to the current collector. However, PVDF is expensive (around 18 Euro kg^{-1}) and hampers easy end of life recycling. Moreover, NMP, which is not only expensive but also toxic and environmentally harmful, is a major drawback for the use of these binder materials. Recently, other binding agents have been recognized as environmentally friendly substitutes of fluorinated polymers. Cellulose derivatives, for instance sodium carboxymethyl cellulose (Na-CMC, or CMC), have attracted great attention as they are not only green materials, but also abundant, cheap (around 1–2 Euro kg^{-1}), and processable in water, thus avoiding the use of volatile organic solvents [16–18]. Furthermore, the use of CMC as binder provides the opportunity to avoid the calendaring of the coated electrodes, which is mandatory when fluorinated binders are used in order to increase the adhesion and compactness of the laminated electrode. Avoiding the calendering step with CMC as binder is possible because CMC shrinks considerably upon finally drying of the electrodes at elevated temperature [19,20]. CMC, or a combination of CMC and styrene butadiene rubber (SBR), has been successfully used already for graphite and silicon based anodes [16,17,21–24]. Recently, Mancini et al. [25] have investigated the use of CMC as binder for anatase TiO_2. The electrodes showed an enhanced compactness relatively to PVDF based electrodes and an improved electrochemical performance. With respect to the cathode side, CMC has also been successfully introduced as a suitable binder for $LiFePO_4$ (LFP) [19], demonstrating the possibility of aqueous processing for LFP based electrodes. Moreover, Li et al. [26] have reported, for the first time, CMC as binder for the high voltage cathode material Li_2MnO_3–$LiMO_2$ (M = Ni, Mn, Co), confirming the stability of this polymer also at voltages as high as 4.8 V. Following this trend, recently, a safer and greener lithium-ion battery, with very promising electrochemical performance, comprising $LiFePO_4$ and $Li_4Ti_5O_{12}$ electrodes, both prepared by using CMC as binder, and an ionic liquid based electrolyte, has been reported [20].

In this context, we report herein our investigation on the use of CMC and CMC/SBR mixtures as binding agent for nanocrystalline anatase TiO_2. The electrochemical performance of TiO_2–CMC and TiO_2–CMC/SBR is compared with those of PVDF and PVDF-HFP based electrodes with and without applying the pressing step. Furthermore, CMC-based NMC electrodes have been prepared and successfully combined with a TiO_2–CMC anode to obtain a fully CMC-based lithium-ion cell. To the best of our knowledge, this is the first report on a full cell comprising CMC-based anatase TiO_2 and NMC electrodes. The electrochemical performance of this full cell presents a promising starting point for further investigation and possible future commercialization of this battery chemistry.

2. Experimental section

2.1. Preparation of TiO_2 electrodes

Nanocrystalline anatase TiO_2, kindly provided by SACHTLEBEN CHEMIE (Hombikat N100, BET surface area = 100 m^2 g^{-1}, particle size (d_{50}) = 2 μm, crystallite size = 20 nm, density = 4.1 g cm^{-3}), was used as received. Four different polymeric binder materials were used for the electrode preparation: (i) PVDF (Kynar Flex 761, ARKEMA), (ii) PVDF-HFP (Kynar Flex 2801, ARKEMA), (iii) Na-CMC (Walocel CRT 2000PA), and (iii) SBR (Lipaton SB5521 50 wt.% water suspension). The fluorinated binders (i) and (ii) were dissolved in NMP (ALDRICH) to obtain solutions containing 10 wt.% of either PVDF or PVDF-HFP. Na-CMC was dissolved in deionized water by continuous magnetic stirring for 1 h at room temperature, to obtain a 5 wt.% solution. For the CMC/SBR mixture (weight-ratio: 7:3) the SBR suspension was added to the 5 wt.% solution of CMC and dispersed by continuous magnetic stirring for 1 h at room temperature. Anatase TiO_2, conductive carbon (Cnergy, Super C65, TIMCAL), and one of the four binder solutions were mixed for 2 h at 800 rpm by means of planetary ball-milling (zirconia balls, balls:-slurry weight ratio 16.2:1, Vario-Planetary Mill Pulverisette 4, FRITSCH). The resulting slurries were immediately casted on dendritic copper foil (SCHLENK) using a laboratory scale doctor blade set to a wet film thickness of 130 μm. Subsequently, the electrodes were pre-dried in oven for 2 h at 80 °C and then left at room temperature overnight. The final composition of the electrodes was 80 wt.% TiO_2, 10 wt.% Super C65, and 10 wt.% binder. Circular electrodes with a diameter of 12 mm were punched and subsequently dried for 12 h at 120 °C (PVDF and PVDF-HFP) or 180 °C (CMC) under vacuum. Some electrodes were additionally pressed at 6 tons cm^{-2}. The average electrodes mass loading was comprised between 1.7 and 2.3 mg cm^{-2}. High resolution scanning electron microscope (HRSEM) analysis on the as prepared electrodes has been carried out on a ZEISS Auriga® microscope.

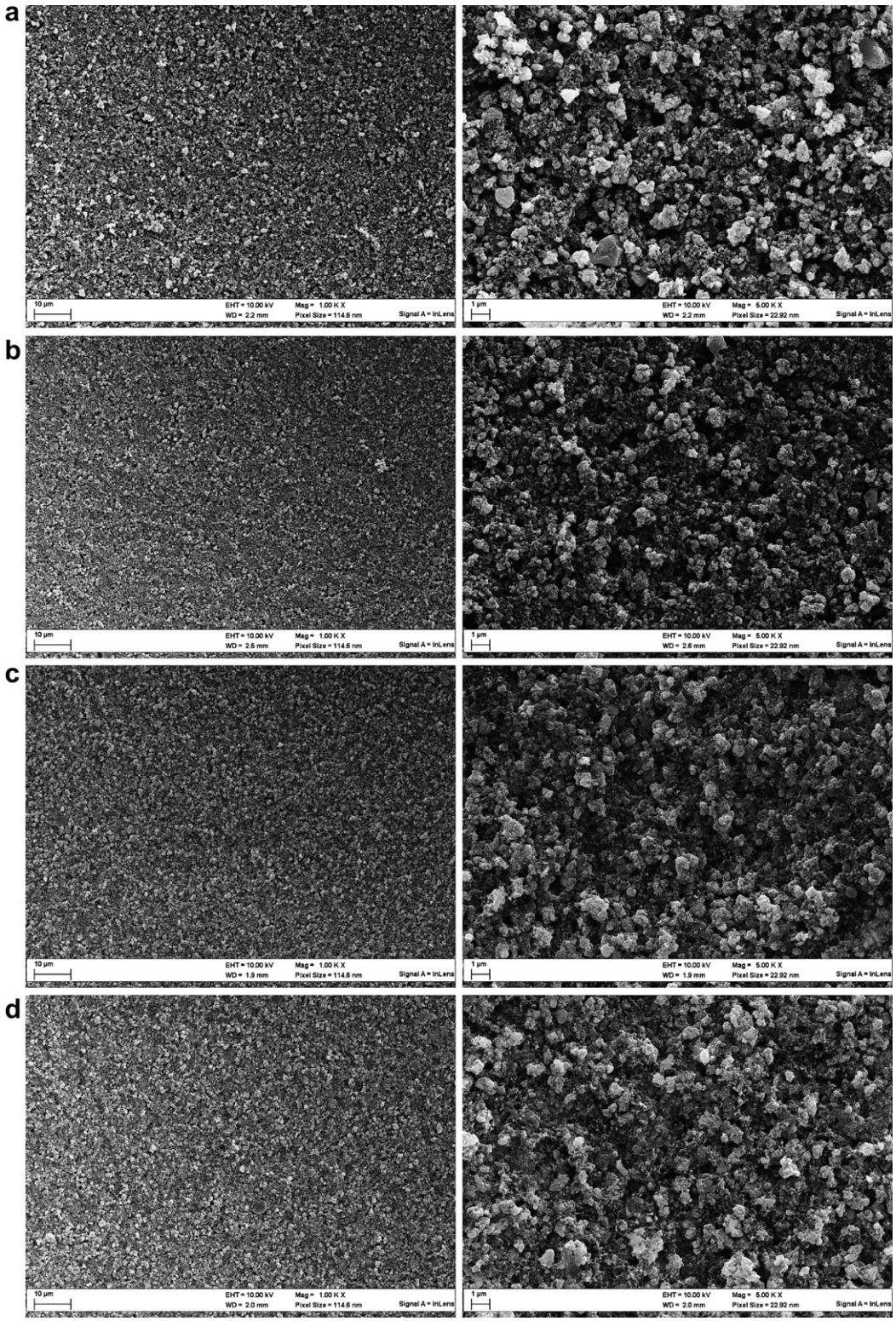

Fig. 1. HRSEM images of TiO_2 based electrodes at different magnifications comprising a) PVDF, b) PVDF-HFP, c) CMC, and d) CMC/SBR (7:3) as binder.

2.2. Preparation of $LiNi_{1/3}Mn_{1/3}Co_{1/3}O_2$ electrodes

$LiNi_{1/3}Mn_{1/3}Co_{1/3}O_2$ powder has been used as received (TODA, average particle size of 10 μm) and mixed with CMC solution to form a slurry which was mixed by magnetic stirring for 3 h and subsequently by means of high-speed mixing (Ultra-Turrax, IKA T25) for 7 min at 5000 rpm. Upon mixing, 0.025 g of formic acid per gram of active material was added to the slurry to prevent the corrosion of the aluminum foil used as electrode current collector. The slurry was casted on the aluminum foil (20 μm, purity >99.9%) by using a laboratory scale doctor blade coater (wet film thickness = 150 μm). The coated aluminum foils were immediately pre-

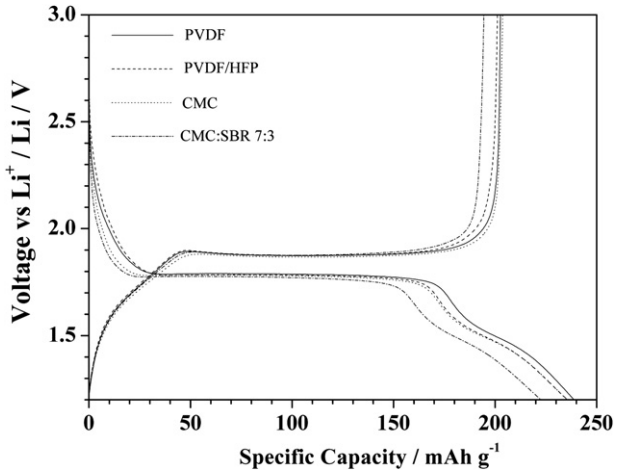

Fig. 2. First cycle voltage profiles (C/20) of non-pressed TiO_2 electrodes comprising different binder materials.

dried in an atmospheric oven at 80 °C for 2 h. Subsequently, electrode discs with a diameter of 12 mm were punched and dried at 180 °C under vacuum for 12 h. The final composition of the resulting $LiNi_{1/3}Mn_{1/3}Co_{1/3}O_2$ electrodes was 88 wt.% NMC, 7 wt.% Super C65, and 5 wt.% CMC and the average electrodes mass loading was 2.65 mg cm^{-2}.

2.3. Electrochemical characterization

Electrochemical measurements on half and full cells were conducted by using three-electrode Swagelok™-type cells. Lithium metal foil (CHEMETALL, lithium battery grade) as counter and reference electrode was used in the case of anatase TiO_2 and NMC half cells. The cells have been assembled in an MBraun glove box with an oxygen and water content below 1 ppm. Whatman GF/D glass fiber disks soaked with 140 μl of 1 M $LiPF_6$ in a 1:1 mixture of ethylene carbonate and dimethyl carbonate (UBE) were used as separator.

All cells were left at OCV for 12 h before running galvanostatic charge–discharge tests at different C rates (room temperature) using a Maccor Battery Tester 4300. For the electrochemical characterization of anatase TiO_2/NMC full cells the electrodes were balanced according to an NMC/TiO_2 ratio of around 1.4 by weight and hence the cells were anode limited. For anatase TiO_2 electrodes the C rate of 1 C corresponded to an applied current of 335 mA g^{-1}, according to a (de-) insertion of 1 lithium per formula unit of TiO_2 per hour. For NMC based electrodes, a 1 C rate corresponds to an applied current of 160 mA g^{-1}. Anatase TiO_2 and NMC half cells were cycled in a voltage range of 1.2–3.0 V and 4.3–3.0 V as cut-off potentials, respectively. For the anatase TiO_2/NMC full cell 0.5 V and 3.1 V *vs.* Li^+/Li have been selected as cut-off potentials. Since in all cases lithium metal was used as reference electrode all potential values within this manuscript are given *vs.* Li^+/Li.

Table 1
First cycle irreversible capacity loss (ICL) at C/20, specific discharge capacity at different C rates and capacity loss per cycle for subsequent cycling at C/2 (from cycle 43 to 150).

Binder	ICL (mAh g^{-1})	Discharge capacity (mAh g^{-1})				Capacity loss (% per cycle)
		C/2	1 C	2.5 C	5 C	
PVDF	40.1	163.4	135.8	101.6	75.2	0.23
PVDF-HFP	34.4	159.7	124.7	78.6	39.2	0.59
CMC	31.6	172.4	160.5	143.3	125.9	0.033
CMC/SBR	28.0	160.6	147.8	127.4	109.0	0.047

3. Results and discussion

Fig. 1(a–d) shows the SEM images of TiO_2 electrodes prepared with the four different binders. All SEM images show a rather homogenous active material distribution. However, for those electrodes comprising fluorinated binders (PVDF and PVDF-HFP) several deeper pores where observed, likely originating from solvent evaporation.

In Fig. 2 the voltage profile of the first cycle at C/20 rate of the non-pressed electrodes based on the four different binders, are presented. In general, all the electrodes show the characteristic features of nanocrystalline anatase TiO_2 upon lithiation (discharge) and subsequent delithiation (charge). Firstly, within the potential region between the initial OCV and approximately 1.8 V a rather sloping voltage profile indicates a solid solution domain, corresponding to an initial lithium insertion in the anatase TiO_2 host structure up to around $Li_{0.09}TiO_2$, in which the anatase phase is still retained. The main plateau at *ca.* 1.8 V corresponds to the first phase transition from lithium poor anatase, space group $I4_1/amd$, to lithium rich titanate, space group *Imma*, resulting in a composition of around $Li_{0.5}TiO_2$. After this main voltage plateau the potential drops again, and at *ca.* 1.5 V a second plateau is observed, corresponding to the second phase transition from lithium rich titanate to a second anatase phase (Li_1TiO_2, space group $I4_1/amd$), for which, however, the formation is limited to a thickness of 4 nm at the TiO_2 particles surface [11,13,27]. As can be seen in Fig. 2 and summarized in Table 1, electrodes containing CMC or CMC/SBR show a slightly reduced irreversible capacity loss (ICL) in the first cycle compared to those containing PVDF or PVDF-HFP as binder. Similar results for anatase TiO_2 based electrodes have been reported already by Mancini et al. [25], and are in line with previous results for carbon and silicon based anodes comprising CMC [22,23]. The nature of the irreversible capacity during the first cycle has been studied by El Ouatani et al. [28] for CMC and CMC/SBR graphite electrodes. They reported a spontaneous reaction of CMC toward the electrolyte probably due to the presence of hydroxide groups at the surface leading to the formation of a surface film, whose presence appears to be beneficial with respect to the first cycle behavior. Based on these results it is likely to suppose that similar reactions are present also in the case of our CMC-based electrodes. The irreversible capacity of TiO_2–CMC/SBR is similar to that of TiO_2/CMC electrodes. However, the reversible capacity is also slightly lower consistently with the insulating properties of SBR [29] which leads to the generation of partially electrochemically inactive areas. A better optimization of the CMC/SBR ratio might lead to a further improved performance.

Fig. 3 shows the rate capability trend for the non-pressed electrodes while Table 1 summarizes the relevant capacity values. TiO_2–CMC and TiO_2–CMC/SBR have higher specific capacity and an enhanced cycling stability at elevated C rates. Particularly, CMC based electrodes show a superior electrochemical performance with a coulombic efficiency higher than 99.9% (Fig. 3, upper panel). The capacity fading of PVDF-HFP based electrodes is more pronounced than that of PVDF based ones. The effect is probably due to the better mechanical strength of PVDF compared to PVDF-HFP. The improved electrochemical performance of CMC and CMC/SBR based electrodes results also from the significantly reduced capacity loss per cycle. The comparison of the voltage profiles of the four kind of electrodes at different C rates (Fig. 4a–d) indicates that the superior electrochemical performance of CMC based electrodes, particularly for elevated C rates, arise from a reduced polarization. These results are in line with those reported earlier by Guyomard

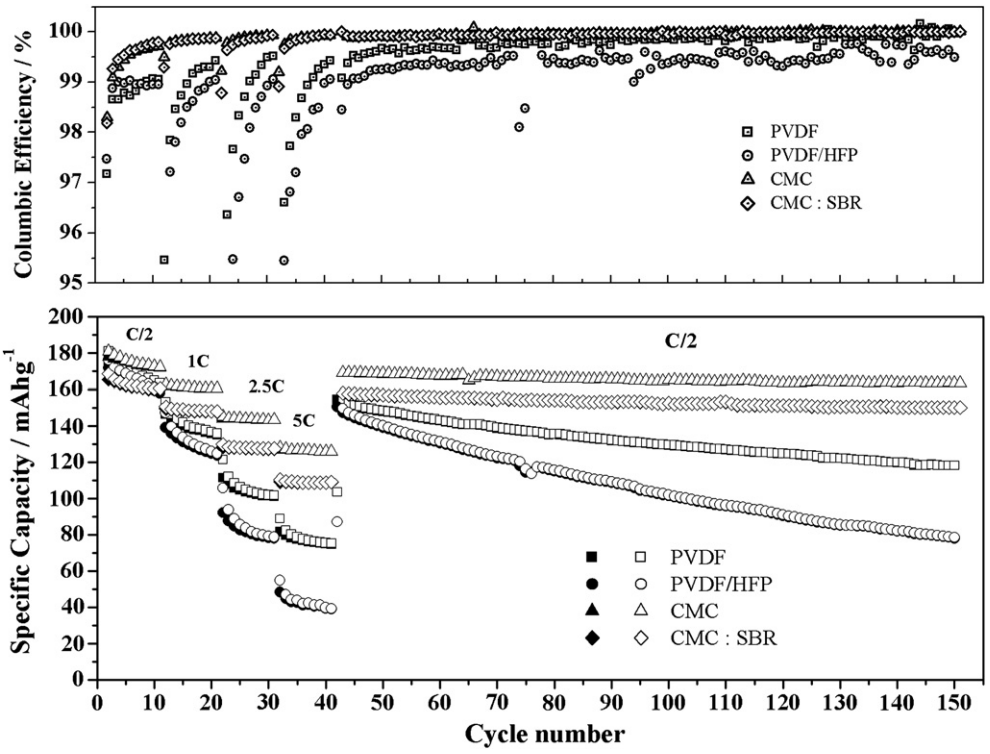

Fig. 3. Bottom panel: specific charge (filled markers) and discharge (hollow markers) capacity at different C rates for TiO_2 based electrodes comprising different binder materials. Upper panel: coulombic efficiency (solid dots) for the same electrodes. Non-pressed electrodes.

and coworkers [30]. These authors attributed the reduced polarization to the improved active material and conductive agent dispersion in CMC-based slurries, which leads to an enhanced electron conductivity. Nevertheless, as CMC is a rather stiff and brittle binder, the addition of a more flexible and elastomeric binder, such as SBR, is required when increasing the mass loading of the electrodes. This determines a slight decrease of the electrochemical properties and further investigation on the appropriate

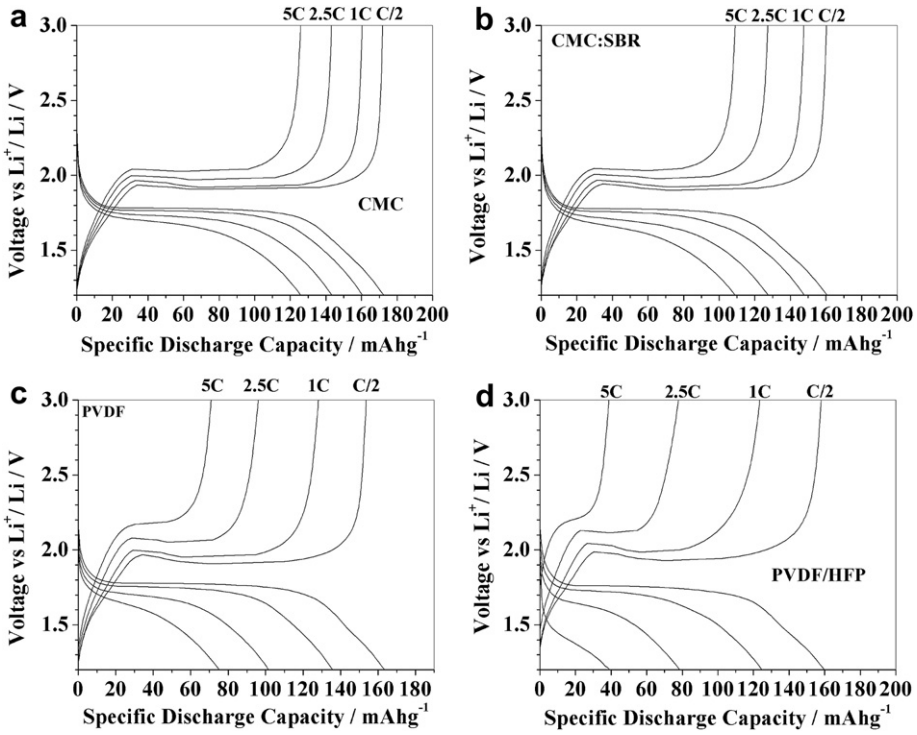

Fig. 4. Voltage profiles *vs.* specific capacity for TiO_2 based electrodes comprising a) CMC, b) CMC/SBR (7:3), c) PVDF, and d) PVDF-HFP as binder.

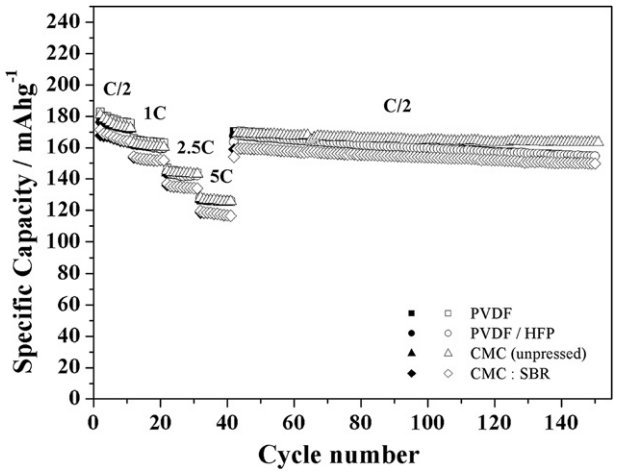

Fig. 5. Specific charge (filled markers) and discharge (hollow markers) capacities at different C rates for pressed TiO_2 based electrodes comprising different binder materials. For sake of comparison also non-pressed CMC electrodes are reported. 1st cycle not shown.

ratio of CMC:SBR is needed to take full advantage from the combination of these two polymers to optimize the performance of TiO_2 based electrodes.

Pressing of electrodes is routinely used in industrial process as it is known to improve the electrochemical performance and cycling stability, particularly for electrodes prepared using fluorinated binder materials. Hence, in Fig. 5 the trend of rate capability of pressed TiO_2–PVDF, TiO_2–PVDF-HFP, and TiO_2–CMC/SBR electrodes (applied pressure 6 tons cm^{-2}) together with those of non-pressed TiO_2–CMC electrodes is presented. Specific discharge capacities, as well as overall capacity loss, are summarized in Table 2. As expected, the electrochemical performance in terms of high rate capability, specific capacity, and coulombic efficiency of TiO_2–PVDF and TiO_2–PVDF-HFP electrodes is significantly improved. The relevant values are comparable to those of non-pressed TiO_2–CMC electrodes. Electrodes comprising a mixture of CMC and SBR also show a slight improvement of the delivered specific capacity. However, the cycling stability of non-pressed CMC based electrodes is still clearly superior as highlighted in Fig. 5, showing a lower capacity fading upon long-term cycling at C/2. These results demonstrate that the compression step appears to be advantageously but not mandatory for aqueous processed TiO_2 electrodes, while it is essential for those comprising fluorinated binders.

Full cells have been studied combining TiO_2 electrodes with NMC as cathode material. As mentioned earlier, the use of a high potential cathode in combination with anatase is required to achieve reasonable values of the overall energy density of the cell. In order to reduce the environmental impact of this cathode material, also NMC based electrodes have been prepared by an aqueous process utilizing CMC as binder. The high rate capability of such aqueous processed NMC electrode *vs.* lithium metal as counter

Table 2
Specific discharge capacity at different C rates and total capacity loss for subsequent cycling at C/2 (from cycle 43 to 150).

Binder	Discharge capacity (mAh g^{-1})				Capacity loss (%)
	C/2	1 C	2.5 C	5 C	
PVDF	175.5	163	143.5	125.4	9.5
PVDF-HFP	172.4	159.9	142.4	126.1	8.1
CMC/SBR	163.3	152.0	134.0	116.6	5.9
CMC	172.4	160.5	143.3	125.9	3.3

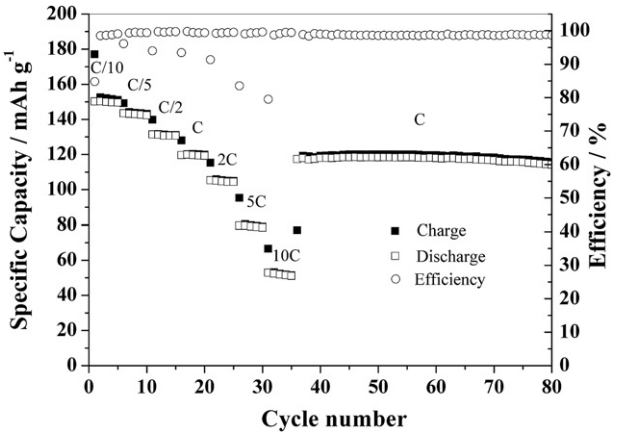

Fig. 6. Galvanostatic (dis-)charge tests at different C rates for a $LiNi_{1/3}Mn_{1/3}Co_{1/3}O_2$ based electrode comprising CMC as binder.

electrode is presented in Fig. 6. The ICL at C/10 is 26.88 mAh g^{-1} and the first cycle coulombic efficiency is 84.8%. The coulombic efficiency increases rapidly upon subsequent cycles and reaches 99% for the 5th cycle with a specific discharge capacity of 150 mAh g^{-1}. At 1 C the specific capacity is around 120 mAh g^{-1}. Nevertheless, with increasing charge–discharge rates the specific capacity decreases to 52 mAh g^{-1} (10 C). However, when the C rate is subsequently decreased again to 1 C, the full initial specific capacity can be recovered. In Fig. 7 the voltage profiles for the 1st, 2nd, and 5th cycle at C/10 are presented. The curves show the characteristic slopy profile of layered NCM. Thus, it can be concluded, that the aqueous processing of NMC as active material does not have any obvious negative effect on its overall electrochemical performance, although recently published aging studies on NMC exposed to H_2O have reported a decrease of performance [31]. A more detailed study on NMC based electrodes comprising CMC as binder will be addressed in a forthcoming communication.

Based on the promising results obtained for TiO_2 and NMC electrodes containing CMC as binder, both electrodes have been combined to a lithium-ion full cell (Fig. 8a–c). The full cell has been balanced according to an NMC:TiO_2 ratio of 1.4 (3.038:2.096 mg of active material) in order to compensate the irreversible capacity loss in the first cycles and to permit the study of the anatase TiO_2 electrode without incurring in cathode limitation problems. The cycling performance of the resulting full cell is presented in Fig. 8a.

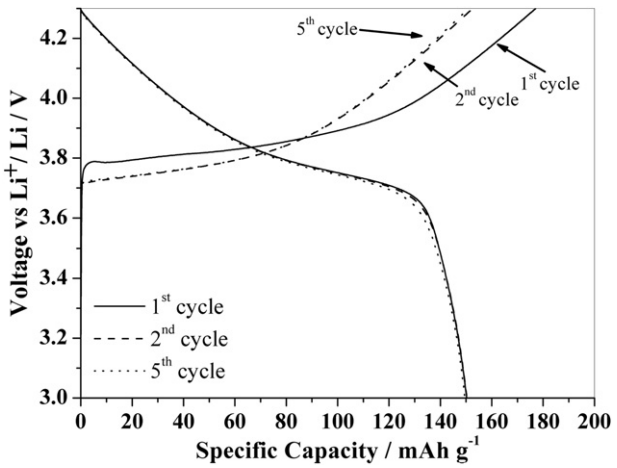

Fig. 7. Voltage profile *vs.* specific capacity of a $LiNi_{1/3}Mn_{1/3}Co_{1/3}O_2$ (NMC) based electrode at C/10 for the 1st, 2nd, and 5th cycle.

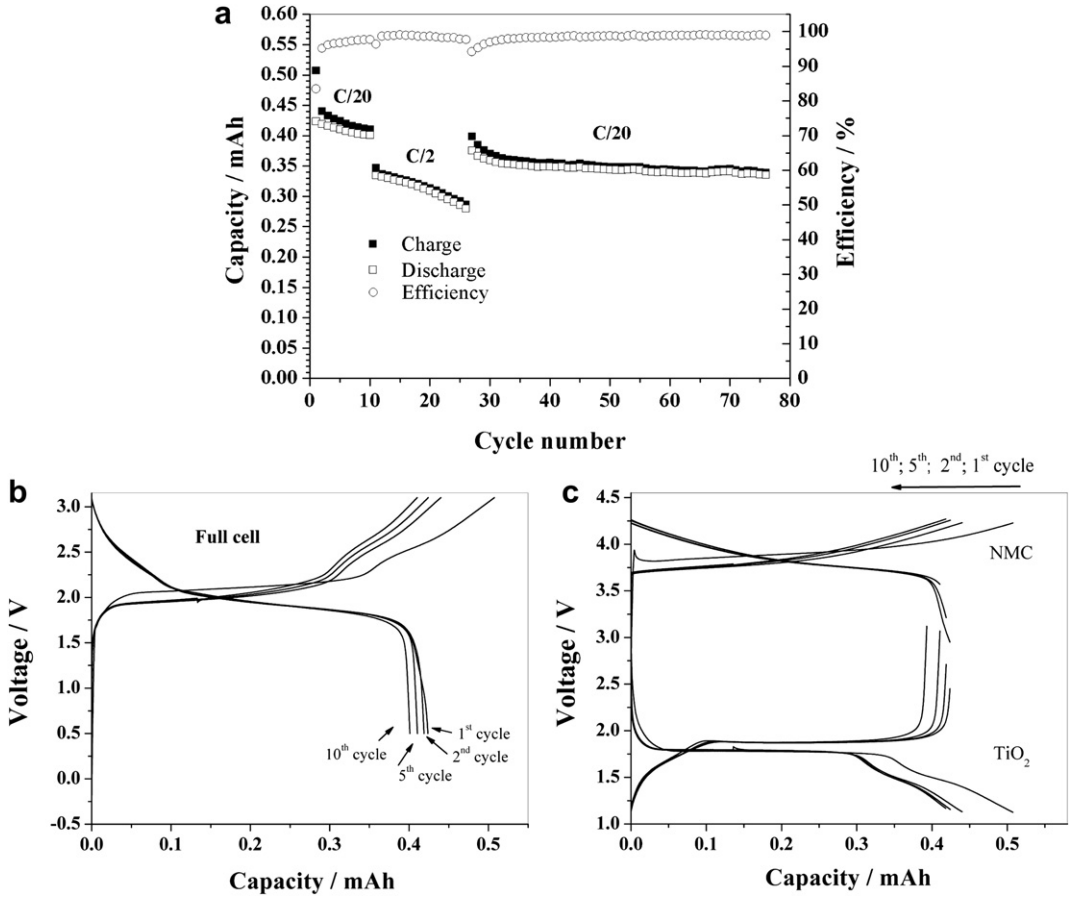

Fig. 8. TiO_2/NMC full cell subjected to galvanostatic (dis-)charge tests at different C rates. a) Capacity of the full cell. b) Voltage profile *vs.* capacity of a full cell at the 1st, 2nd, 5th, and 10th cycles. c) Voltage profile *vs.* capacity of the two electrodes (TiO_2 and NMC) at the 1st, 2nd, 5th, and 10th cycles.

For the first cycle (C/20) a discharge capacity of 0.424 mAh and a coulombic efficiency of 83% is obtained in good agreement with the first cycle efficiency observed for TiO_2 electrodes in half cells. A few selected voltage profiles of the cell and individual electrodes are shown in Fig. 8b and c. An initial slight decrease in capacity is observed. At the 10th cycle (C/20) a capacity of 0.401 mAh is obtained, corresponding to a specific capacity for the TiO_2 anode of 191 mAh g^{-1} with a coulombic efficiency of around 98%. In the first cycle at C/2 (Fig. 8a), the cell still delivers a capacity of 0.334 mAh, corresponding to a specific capacity of 159 mAh g^{-1} and 110 mAh g^{-1} for the TiO_2 anode and the NCM cathode, respectively, resulting in a total energy density of 120.56 Wh kg^{-1} for the full cell (calculated on the base of the overall mass of active material of both electrodes). Upon continuous cycling of the cell at C/2 a capacity fading is observed resulting in a capacity value of 0.280 mAh at the 26th cycle. However, when the C rate is decreased again to C/20 (27th cycle), the whole capacity of the 10th cycle – the last cycle at C/20 – is recovered, and becomes rather stable during the following cycles at a value of about 0.340 mAh. Hence, it is concluded that the rather pronounced capacity decrease at elevated C rate (C/2) can be ascribed to kinetic reasons rather than to irreversible processes.

4. Conclusion

The influence of different binding agents on the electrochemical performance of nanocrystalline anatase TiO_2 has been investigated. It has been demonstrated that TiO_2 electrodes comprising CMC or a CMC/SBR mixture as binder material show an enhanced electrochemical performance with respect to those based fluorinated binders, enabling the preparation of environmentally friendly electrodes for cheaper lithium-ion batteries. The aqueous processing of such electrodes as well as the opportunity to avoid an additional pressing step allows a more cost-efficient and greener electrode preparation process. Moreover, the possible combination with CMC based NMC electrodes, which – to the best of our knowledge – is herein presented for the first time, results in 2.6 V lithium-ion cell with an energy density of more than 120 mWh g^{-1}. The results demonstrate a proof-of-concept and a promising starting point, stimulating further investigation for the development of a completely NMP and fluorine free lithium-ion electrode preparation.

Acknowledgment

Financial support from the European Commission in the ORION project (229036) under the Seventh Framework Programme (7th FWP) is gratefully acknowledged. Furthermore, the authors want to thank Sachtleben Chemie GmbH for providing the investigated sample of anatase TiO_2.

References

[1] B. Scrosati, J. Garche, Journal of Power Sources 195 (2010) 2419.
[2] C.H. Doh, D.H. Kim, H.S. Kim, H.M. Shin, Y.D. Jeong, S.I. Moon, B.S. Jin, S.W. Eom, H.S. Kim, K.W. Kim, D.H. Oh, A. Veluchamy, Journal of Power Sources 175 (2008) 881.
[3] E. Peled, Journal of the Electrochemical Society 126 (1979) 2047.

[4] R. Yazami, Electrochimica Acta 45 (1999) 87.
[5] G.N. Zhu, Y.G. Wang, Y.Y. Xia, Energy and Environmental Science 5 (2012) 6652.
[6] Z. Yang, D. Choi, S. Kerisit, K.M. Rosso, D. Wang, J. Zhang, G. Graff, J. Liu, Journal of Power Sources 192 (2009) 588.
[7] B. Zachau-Christiansen, K. West, T. Jacobsen, S. Atlung, Solid State Ionics 28-30 (1988) 1176.
[8] T. Ohzuku, T. Kodama, T. Hirai, Journal of Power Sources 14 (1985) 153.
[9] L. Kavan, M. Gratzel, S.E. Gilbert, C. Klemenz, H.J. Scheel, Journal of American Chemical Society 118 (1996) 6716.
[10] G. Sudant, E. Baudrin, D. Larcher, J.M. Tarascon, Journal of Material Chemistry 15 (2005) 1263.
[11] M. Wagemaker, W. Borghols, F.M. Mulder, Journal of American Chemical Society 129 (2007) 4323.
[12] M. Wagemaker, W.J.H. Borghols, E.R.H. van Eck, A.P.M. Kentgens, G.J. Kearley, F.M. Mulder, Chemistry – A European Journal 13 (2007) 2023.
[13] D. Bresser, E. Paillard, E. Binetti, S. Krueger, M. Striccoli, M. Winter, S. Passerini, Journal of Power Sources 206 (2012) 301.
[14] P. Reale, D. Privitera, S. Panero, B. Scrosati, Solid State Ionics 178 (2007) 1390.
[15] V. Etacheri, R. Marom, R. Elazari, G. Salitra, D. Aurbach, Energy and Environmental Science 4 (2011) 3243.
[16] F.M. Courtel, S. Niketic, D. Duguay, Y. Abu-Lebdeh, I.J. Davidson, Journal of Power Sources 196 (2011) 2128.
[17] J. Drofenik, M. Gaberscek, R. Dominko, F.W. Poulsen, M. Mogensen, S. Pejovnik, J. Jamnik, Electrochimica Acta 48 (2003) 883.
[18] S.S. Jeong, N. Bockenfeld, A. Balducci, M. Winter, S. Passerini, Journal of Power Sources 199 (2012) 331.
[19] S.F. Lux, F. Schappacher, A. Balducci, S. Passerini, M. Winter, Journal of the Electrochemical Society 157 (2010) A320.
[20] G.T. Kim, S.S. Jeong, M. Joost, E. Rocca, M. Winter, S. Passerini, A. Balducci, Journal of Power Sources 196 (2011) 2187.
[21] J.H. Lee, U. Paik, V.A. Hackley, Y.M. Choi, Journal of the Electrochemical Society 152 (2005) A1763.
[22] H. Buqa, M. Holzapfel, F. Krumeich, C. Veit, P. Novak, Journal of Power Sources (2006) 161.
[23] J. Li, R.B. Lewis, J.R. Dahn, Electrochemical and Solid-state Letters 10 (2007) A17.
[24] W.R. Liu, M.H. Yang, H.C. Wu, S.M. Chiao, N.L. Wu, Electrochemical and Solid-state Letters 8 (2005) A100.
[25] M. Mancini, F. Nobili, R. Tossici, M. Wohlfahrt-Mehrens, R. Marassi, Journal of Power Sources 196 (2011) 9665.
[26] J. Li, R. Klopsch, S. Nowak, M. Kunze, M. Winter, S. Passerini, Journal of Power Sources 196 (2011) 7687.
[27] U. Lafont, D. Carta, G. Mountjoy, A.V. Chadwick, E.M. Kelder, Journal of Physical Chemistry C 114 (2010) 1372.
[28] L. El Outani, R. Dedryvère, J.-B. Ladeuil, C. Siret, P. Biensan, J. Desbrières, D. Gonbeu, Journal of Power Sources 189 (2009) 72.
[29] J. Chong, S. Xun, H. Zheng, X. Song, G. Liu, P. Ridgway, J.Q. Wang, V.S. Battaglia, Journal of Power Sources 196 (2011) 77074.
[30] B. Lestriez, S. Bahri, I. Sandu, L. Roué, D. Guyomard, Electrochemistry Communication 9 (2007) 2801.
[31] X. Zhang, W.J. Jiang, X.P. Zhu, A. Mauger, Qilu, C.M. Julien, Journal of Power Sources 196 (2011) 5102.